Available online at http://jprm.sms.edu.pk/
Journal of Prime Research in Mathematics, 2026, 101–118

Journal of Prime Research in Mathematics

Numerical Analysis of the Coupled Fractional Whitham-Broer-Kaup System

Shravan Lal Nitharwal[a], Ekta Mittal[a], Manjeet Kumari[b], Sunil Dutt Purohit[c,*]

[a]*Department of Mathematics, IIS (Deemed to be University), Jaipur, India.*
[b]*Department of Mathematics, St. Xavier College, Nevta, Jaipur, India.*
[c]*Department of HEAS (Mathematics), Rajasthan Technical University, Kota, Rajasthan, India.*

Abstract

In the current study, we derive the analytical solution of applications of Coupled modified Boussinesq and approximate long wave equations, a significant mathematical model for representing wave propagation in shallow water. The solution is obtained through the utilization of the q-homotopy analysis Shehu transform method (q-HASTM), a hybrid approach combining Shehu transformation and the q-homotopy analysis method. Homotopy polynomials are employed to address non-linear terms, and the introduced algorithm incorporates the auxiliary parameter $\hbar$ and n to regulate the convergence region of the resulting series solution. Comparative numerical analyses are conducted with outcomes from the Adomian decomposition method (ADM), variational iteration method (VIM), optimal homotopy asymptotic method (OHAM) and residue power series method (RPSM), demonstrating the superior accuracy of the proposed method. The method's novelty and straightforward implementation establish it as a reliable and efficient analytical technique for solving both linear and non-linear fractional partial differential equations.

Keywords: Coupled modified Boussinesq and approximate long wave equations, homotopy analysis method, Shehu transform, Caputo fractional derivative.
2010 MSC: 26A33.

1. Introduction

Fractional calculus in its modern and most widely studied form was motivated by a question L'Hospital asked Gottfried Wilhelm Leibniz in 1695. L'Hopital asked what was the meaning of a derivative of order $\eth = \frac{1}{2}$ and the question led to the beginnings of the great new field of fractional calculus. A relationship between fractional calculus, and specifically the interplay between fractional calculus and symmetry has become a topic of interest in the last few decades to researchers in a range of fields of study. This has led to the increased interest which is supported by the fact that it has capability of modeling and interpreting

*Corresponding author
Email addresses: slnitharwal7292@gmail.com (Shravan Lal Nitharwal), ekta.mittal@iisuniv.ac.in (Ekta Mittal), manjeetkumari@sxcjpr.edu.in (Manjeet Kumari), sunil_a_purohit@yahoo.com (Sunil Dutt Purohit)

Received : 15 October 2026*; Accepted:* 22 March 2026*; Published Online:* 29 March 2026

a great number of nonlinear and complicated phenomena accurately. Fractional-order differential equations (FDEs) generalize classical differential equations by considering non-locality and memory effects that are essential to model the intrinsic behavior of many natural and man made systems. Many researchers have contributed greatly to the theory of fractional calculus proposing the generalized definitions of derivatives and integrals of an arbitrary order. Such developments have preconditioned a very robust mathematical base, which allows developing and understanding new types of differential equations. In nonlinear problem solving, FDEs are playing a more and more predominant role in both analytical and numerical methods. These solutions play the crucial role in the study of the dynamic properties of complex systems that are found in applied mathematics and many areas of technology. Nevertheless, obtaining specific analytical solutions turns out to be a major challenge. To eliminate this issue, the methods of integral transform were developed, which can be described as potent and multi-purpose tools since they simplify and solve such equations. The methods have been widely used in many fields of science such as biology [11, 39, 44], electrodynamics [30], continuum mechanics [10], nanotechnology [5], biotechnology [24], chaos theory [6, 7], and many others [1, 3, 14, 32, 36, 40]. Its further evolvement and use prove the vitality of the fractional calculus in developing the both theoretical and applied sciences.

In recent years, a wide range of analytical and numerical approaches have been developed and employed to solve fractional-order differential equations. Notable among these are the Shehu transform decomposition method [43], homotopy analysis transform method [22], the generalized Riccati method [38], Adomian decomposition method [33], homotopy analysis shehu transform method (HASTM) [23], Coupled FCT-HP method [12], fractional iteration method [29], and fractional residue power series method [35] and others [19, 31, 4, 9]. In addition to these, integral transforms play a pivotal role in solving integral and delay differential equations, providing a powerful mathematical toolset for simplifying complex problems. When appropriately chosen, these transforms enable the reduction of differential and integral equations to simpler algebraic forms. The historical roots of integral transforms can be traced back to the foundational work of P.S. Laplace in the 1780s and Joseph Fourier in 1822. Among the most widely used, the Laplace and Fourier transforms were originally introduced for solving ordinary and partial differential equations and continue to be central in modern analytical methods.

In recent years, several novel integral transforms have been introduced by researchers to address various types of mathematical systems, including the Elzaki transform, the ρ-Laplace transform, the Sumudu transform, the generalized Laplace transform, and the Natural transform [21], Upadhyaya transform [18] and new general integral transform [28, 17]. The Shehu transform, in particular, offers several key advantages over the traditional Laplace transform, especially when applied to fractional differential equations. Its dual-parameter structure (v, μ) provides greater flexibility in adjusting the kernel $\exp(-v\tau/\mu)$, enabling better adaptation to oscillatory, exponential, and fractional behaviors without requiring complex contour integrations in certain cases. By setting $\mu = 1$, it reduces directly to the Laplace transform, while specific choices of μ yield the Sumudu transform, ensuring compatibility with existing methods. This parameterization often leads to simpler algebraic manipulations in the transform domain and easier inversion for nonlinear or fractional partial differential equations compared to the standard Laplace approach. The present work employs the Shehu transform as a powerful generalization of both the Laplace and Sumudu transforms. Notably, its structural properties exhibit strong similarities to those of the Natural transform, as established through well-known duality relations that allow inter-conversion by simple parameter substitutions.

The Whitham-Broer-Kaup (WBK) equations describe the propagation of shallow water wave [15], with different dispersion relations. These coupled system was introduced by G. B. Whitham [42], L. J. Broer [8] and D. J. Kaup [20], which are given as

$$\begin{cases} \psi_\tau + \ \psi\,\psi_\varrho + \nu_\varrho + \ b\,\psi_{\varrho\varrho} \ = \ 0, \\ \nu_\tau + \ (\nu\psi)_\varrho + a\,\psi_{\varrho\varrho\varrho} - \ b\,\nu_{\varrho\varrho} \ = \ 0. \end{cases} \tag{1.1}$$

In the preceding equations, $\psi(\varrho, \tau)$ and $\nu(\varrho, \tau)$ indicates the horizontal velocity and height that deviates from the equilibrium position, respectively. The parameters a and b regulate the dispersion and diffusion effects, respectively. a determines the strength of the third-order dispersive term, whereas b influences the

second-order diffusive terms, allowing the model to describe a variety of wave patterns in shallow water, such as solitary waves or wave breaking.
The WBK equations with the fractional Caputo derivative can be rewritten as

$$\begin{cases} {}^{C}D_{\tau}^{\eth}\psi + \ \psi\,\psi_{\varrho} + \nu_{\varrho} + \ b\,\psi_{\varrho\varrho\varrho} \ = \ 0, \\ {}^{C}D_{\tau}^{\eth}\nu + \ (\nu\psi)_{\varrho} + \ a\,\psi_{\varrho\varrho\varrho} - \ b\,\nu_{\varrho\varrho} \ = \ 0. \end{cases} \tag{1.2}$$

where $0 < \varrho \leq 1$ and ${}^{C}D_{\tau}{}^{\varrho}$ present the Caputo fractional derivative of order ϱ. It is noted that for $a = 1$ and $b = 0$, system (1.2) becomes to modified Boussinesq (MB) equations and for $a = 0$ and $b = 1/2$, system (1.2) becomes to approximate long wave (ALW) equations. In last few years, many researches studied these equations with numerous schemes. Recently, past few years numerous researchers took the attention on these equations and obtained the solutions with numerous approaches [2, 13, 34, 37, 41].
In this study, we employ the q-homotopy analysis shehu transform method (q-HASTM) to obtain analytical solutions for the considered systems. The proposed scheme represents an effective integration of the q-homotopy analysis method (q-HAM) and the Shehu transform, combining the strengths of both approaches to address fractional differential equations (FDEs). A key advantage of this method lies in its flexibility: by selecting an appropriate $\hbar$-parameter, the convergence region of the solution series can be effectively controlled over a wide domain. The merits of q-HASTM are numerous. It operates without the need for linearization or discretization, involves minimal perturbation, and imposes no restrictive assumptions. Additionally, it significantly reduces computational complexity, accounts for non-local effects, ensures a large convergence domain, and eliminates the need for complicated polynomial generation, integration procedures, or specific physical parameters.

2. Fractional calculus basic concepts

Definition 2.1. The fractional Caputo derivative of a function $\Im \in C_{-1}^{\varrho}$ with $\varrho \in \mathbb{N} \cup \{0\}$ is given by:

$$D_{\tau}^{\eth}\Im(\tau) = \begin{cases} I^{\varrho-\eth} f^{(\varrho)}, & \varrho - 1 < \eth \leq \varrho, \ \varrho \in \mathbb{N}, \\ \dfrac{d^{\varrho}}{d\tau^{\varrho}}\Im(\tau), & \eth = \varrho, \ \varrho \in \mathbb{N}. \end{cases} \tag{2.1}$$

Definition 2.2. The Mittag–Leffler function (MLF) with two parameters is expressed as [28]

$$E_{\delta,\beta}(\tau) = \sum_{k=0}^{\infty} \frac{\tau^{k}}{\Gamma(k\delta + \beta)}. \tag{2.2}$$

For $\delta = \beta = 1$, $E_{1,1}(\tau) = e^{\tau}$ and $E_{1,1}(-\tau) = e^{-\tau}$.

Definition 2.3. The Shehu transform is a relatively new integral transform that has structural similarities to other well-known integral transforms such as the Laplace and Sumudu transforms. It is developed exclusively for exponential-order functions [27]. Consider the functions belonging to the set A, defined as follows:

$$A = \left\{ \Im(\tau) \;\middle|\; \exists\, M > 0, \ \rho > 0 \text{ such that } |\Im(\tau)| \leq M e^{|\tau|/\rho} \text{ for all } \tau \in \mathbb{R} \right\}.$$

The Shehu transform of a function $\Im(\tau)$, denoted by $S\{\Im(\tau)\}$, is defined for $\tau \geq 0$ and parameters satisfying $\nu > 0$ and $\mu > 0$ as:

$$S\{\Im(\tau)\} = V(\nu, \mu) = \int_{0}^{\infty} \Im(\tau)\, e^{-\frac{\nu\tau}{\mu}}\, d\tau.$$

Here, $V(\nu, \mu)$ represents the Shehu transform of $\Im(\tau)$. Conversely, the inverse Shehu transform, denoted S^{-1}, recovers the original function from its transform:

$$S^{-1}\{V(\nu,\mu)\} = \Im(\tau), \quad \tau \geq 0.$$

Thus, S^{-1} is the inverse Shehu transform operator.

Definition 2.4 (**Shehu transform for n^{th} derivatives**)**.** The Shehu transform of the n^{th} derivative of a function $\Im(\tau)$ is given by

$$S\left\{\Im^{(n)}(\tau)\right\} = \frac{\nu^n}{\mu^n}V(\nu,\mu) - \sum_{k=0}^{n-1}\left(\frac{\nu}{\mu}\right)^{n-k-1}\Im^{(k)}(0), \quad n \in \mathbb{N}, \tag{2.3}$$

where $V(\nu,\mu) = S\{\Im(\tau)\}$ is the Shehu transform of $\Im(\tau)$.

Definition 2.5. The Shehu transformation for the fractional order derivatives is expressed as [27]

$$S\{{}^{C}D_{\tau}^{\eth}\Im(\tau)\} = \frac{\nu^{\eth}}{\mu^{\eth}}V(\nu,\mu) - \sum_{k=0}^{\varrho-1}\left(\frac{\nu}{\mu}\right)^{\eth-k-1}\Im^{(k)}(0), \quad 0 < \eth \leq \varrho, \tag{2.4}$$

where ϱ is a positive integer.

3. q-Homotopy analysis Shehu transform method

To formulate the basic idea of the q-HASTM, we consider the following nonlinear fractional partial differential equation

$$(D^{\eth}\psi)(\varrho,\tau) + R\psi(\varrho,\tau) + N\psi(\varrho,\tau) = g(\varrho,\tau), \quad 0 < \eth \leq 1, \tag{3.1}$$

where N is the nonlinear operator, $(D^{\eth}\psi)(\varrho,\tau)$ is the Caputo fractional derivative, $R\psi(\varrho,\tau)$ is the remaining linear operator, and $g(\varrho,\tau)$ is the source term.

Applying the Shehu transform $\mathcal{S}$ to Eq.(3.1) and after simplification, we get

$$\left(\frac{v}{\mu}\right)^{\eth}\left[\mathcal{S}[\psi(\varrho,\tau)] - \sum_{k=0}^{m-1}\left(\frac{\mu}{v}\right)^{k}\psi^{(k)}(\varrho,0)\right] + \mathcal{S}[R\psi(\varrho,\tau)] + \mathcal{S}[N\psi(\varrho,\tau)] = \mathcal{S}[g(\varrho,\tau)], \tag{3.2}$$

where $m-1 < \eth \leq m$. Equivalently,

$$\mathcal{S}[\psi(\varrho,\tau)] - \left(\frac{\mu}{v}\right)^{\eth}\sum_{k=0}^{m-1}\left(\frac{v}{\mu}\right)^{k+1}v^{(k)}(x,0) + \left(\frac{\mu}{v}\right)^{\eth}\left(\mathcal{S}[R\psi(\varrho,\tau)] + \mathcal{S}[N\psi(\varrho,\tau)] - \mathcal{S}[g(\varrho,\tau)]\right) = 0. \tag{3.3}$$

We define the nonlinear operator as

$$\begin{aligned} N[\Upsilon(\varrho,\tau;q)] = \mathcal{S}[\Upsilon(\varrho,\tau;q)] - \left(\frac{u}{s}\right)^{\eth}\sum_{k=0}^{m-1}\left(\frac{s}{u}\right)^{k+1}\Upsilon^{(k)}(\varrho,0;q) \\ + \left(\frac{u}{s}\right)^{\eth}\Big(\mathcal{S}[R\,\Upsilon(\varrho,\tau;q)] + \mathcal{S}[N\,\Upsilon(\varrho,\tau;q)] - \mathcal{S}[g(\varrho,\tau)]\Big). \end{aligned} \tag{3.4}$$

where $\Upsilon(\varrho,\tau;q)$ is a real-valued function of ϱ, τ, q, and $q \in \left[0,\frac{1}{n}\right]$ denotes the embedding parameter.

We construct the homotopy as follows:

$$(1-nq)\mathcal{S}[\Upsilon(\varrho,\tau;q) - \psi_0(\varrho,\tau)] = hqH(\varrho,\tau)N[\Upsilon(\varrho,\tau;q)], \tag{3.5}$$

where $\mathcal{S}$ denotes the Shehu transform, $q \in \left[0,\frac{1}{n}\right]$ is the embedding parameter, $H(\varrho,\tau)$ denotes a nonzero auxiliary function, $h \neq 0$ is an auxiliary parameter, $\psi_0(\varrho,\tau)$ is the initial guess function, and $\Upsilon(\varrho,\tau;q)$ is the unknown function.

Based on the concept of q-HAM, one has great freedom to choose the auxiliary parameter and the initial guess. Obviously, when $q = 0$ and $q = \frac{1}{n}$ in Eq. (3.5), the following results hold:

$$\Upsilon(x,t;0) = \psi_0(\varrho,\tau), \quad \text{and} \quad \Upsilon(x,t;\frac{1}{n}) = \psi(\varrho,\tau), \tag{3.6}$$

respectively. Thus, as q increases from 0 to $\frac{1}{n}$, the solution $\Upsilon(\varrho,\tau;q)$ varies from the initial guess $v_0(\varrho,\tau)$ to the solution $\psi(\varrho,\tau)$.

Expanding $\Upsilon(\varrho,\tau;q)$ as a Taylor series with respect to p, we deduce

$$\Upsilon(\varrho,\tau;q) = \psi_0(\varrho,\tau) + \sum_{p=1}^{\infty} \psi_p(\varrho,\tau)\, q^p, \tag{3.7}$$

where

$$\psi_p(\varrho,\tau) = \frac{1}{p!} \frac{\partial^p \Upsilon_1(\varrho,\tau;q)}{\partial q^p}\bigg|_{q=0}. \tag{3.8}$$

By proper choosing of $\psi_0(\varrho,\tau)$, $\hbar$, and $H(\varrho,\tau)$, the series in equation (3.7) converges at q = $\frac{1}{n}$, we will get

$$\psi(\varrho,\tau) = \psi_0(\varrho,\tau) + \sum_{p=1}^{\infty} \psi_p(\varrho,\tau) \left(\frac{1}{n}\right)^p. \tag{3.9}$$

We define the vectors as

$$\overrightarrow{\psi_p}(\varrho,\tau) = \{\psi_0(\varrho,\tau),\, \psi_1(\varrho,\tau),\, ...,\, \psi_p(\varrho,\tau)\}. \tag{3.10}$$

First, differentiating equation (3.5) p- times with respect to q, then evaluate at q = 0 and finally dividing by $\Gamma(p+1)$, we get

$$S\left[\psi_p(\varrho,\tau) - \chi_p \psi_{p-1}(\varrho,\tau)\right] = \hbar H(\varrho,\tau) R_p\left[\overrightarrow{\psi}_{p-1}\right], \tag{3.11}$$

where,

$$R_p(\vec{\psi}_{p-1},\varrho,\tau) = \left[\frac{1}{\Gamma(p)} \frac{\partial^{p-1} N[\vartheta(\varrho,\tau;q)]}{\partial q^{\,p-1}}\right]_{q=0}, \tag{3.12}$$

and

$$\chi_p = \begin{cases} 0, & p \le 1 \\ n, & otherwise\ . \end{cases} \tag{3.13}$$

Computing the inverse Shehu transform on both sides of Eq. (3.11) yields

$$\psi_p(\varrho,\tau) = \chi_p \psi_{p-1}(\varrho,\tau) + \mathcal{S}^{-1}\left[hH(\varrho,\tau) R_p(\vec{\psi}_{p-1},\varrho,\tau)\right]. \tag{3.14}$$

Based on Eq. (3.1), $R_p(\vec{\psi}_{p-1})$ is defined as

$$R_p(\vec{\psi}_{p-1},\varrho,\tau) = D^{\eth}\psi_{p-1}(\varrho,\tau) + R\psi_{p-1}(\varrho,\tau) + N\psi_{m-1}(\varrho,\tau) - (1 - \frac{\chi_p}{n}) g(\varrho,\tau). \tag{3.15}$$

Finally, we compute $\psi_p(\varrho,\tau)$ by using equation (3.15) for $p \ge 1$. Hence the M^{th} order approximate solution of equation (3.1) can be represented as

$$\psi(\varrho,\tau) = \psi_0(\varrho,\tau) + \sum_{p=1}^{M} \psi_p(\varrho,\tau) \left(\frac{1}{n}\right)^p. \tag{3.16}$$

Moreover, for $M \to \infty$, we get

$$\psi(\varrho,\tau) = \psi_0(\varrho,\tau) + \sum_{p=1}^{\infty} \psi_p(\varrho,\tau) \left(\frac{1}{n}\right)^p. \tag{3.17}$$

Thus, we obtain the series solution, whose convergence is ensured with the help of the convergence–control parameter $\hbar$ and n. Note that in the q-homotopy analysis method (q-HAM), setting the auxiliary parameter $\hbar = -1$and $n = 1$ reduces the approach to the homotopy perturbation method (HPM), providing a special case for validation against perturbation-based techniques. In the next theorem, we study the convergence analysis of the original problem given in Eq. (3.1).

4. Convergence of the Series Solution

Theorem 4.1. *If the series solution*

$$\sum_{p=0}^{\infty} \psi_p(\varrho,\tau) = \psi_0(\varrho,\tau) + \sum_{p=1}^{\infty} \psi_p(\varrho,\tau)\left(\frac{1}{n}\right)^p, \tag{4.1}$$

is convergent to $\Theta(\varrho,\tau)$*, where* $\psi_p(\varrho,\tau)$ *is generated by the pth-order deformation Eq.* (3.11) *based on Eqs.* (3.12) *and* (3.15)*, then* $\psi(\varrho,\tau)$ *must be the solution of the original problem Eq.* (3.1)*.*

Proof.

$$\lim_{M\to\infty} \sum_{p=0}^{M} \psi_p(\varrho,\tau) = \psi_0(\varrho,\tau) + \lim_{M\to\infty} \sum_{p=1}^{M} \psi_m(\varrho,\tau)\left(\frac{1}{n}\right)^p = \Theta(\varrho,\tau). \tag{4.2}$$

Then we have $\lim_{M\to\infty} \sum_{p=1}^{M} \psi_p(\varrho,\tau) = 0$. Using Eq. (3.11), we get

$$\begin{aligned}
\lim_{M\to\infty} \left[\hbar H(\varrho,\tau) \sum_{p=1}^{M} R_p(\vec{\psi}_{p-1})\right] &= \lim_{M\to\infty} \left[\sum_{p=1}^{M} \mathcal{S}\big(\psi_p(\varrho,\tau) - \chi_p \psi_{p-1}(\varrho,\tau)\big)\right] \\
&= \mathcal{S}\left[\lim_{M\to\infty} \sum_{p=1}^{M} \psi_p(\varrho,\tau) - \lim_{M\to\infty} \sum_{p=1}^{M} \chi_p \psi_{p-1}(\varrho,\tau)\right] \\
&= \mathcal{S}\left[(1-\chi_2) \lim_{M\to\infty} \sum_{p=1}^{M} \psi_p(\varrho,\tau)\right] \\
&= \mathcal{S}\Big[(1-\chi_2)\big(\Theta(\varrho,\tau) - \psi_0(\varrho,\tau)\big)\Big],
\end{aligned}$$

which yields, since $H(\varrho,\tau) \neq 0$, $h \neq 0$ and the linearity property of Eq. (3.5), we get

$$\lim_{M\to\infty} \sum_{p=1}^{M} R_p(\vec{\psi}_{p-1}) = 0. \tag{4.3}$$

Similarly, based on Eq. (3.15), we deduce

$$\begin{aligned}
\lim_{M\to\infty} \sum_{p=1}^{M} R_p(\vec{\psi}_{p-1}) &= \lim_{M\to\infty} \sum_{p=1}^{M} \Big[D^{\eth}\psi_{p-1}(\varrho,\tau) + R\psi_{p-1}(\varrho,\tau) + N\psi(\varrho,\tau)_{p-1} - (1-\frac{\chi_p}{n})g(\varrho,\tau)\Big] \\
&= D^{\eth} \lim_{M\to\infty} \sum_{p=1}^{M} \psi_{p-1}(\varrho,\tau) + \lim_{M\to\infty} \sum_{p=1}^{M} R\psi_{p-1}(\varrho,\tau) \\
&\quad + \lim_{M\to\infty} \sum_{p=1}^{M} N\psi(\varrho,\tau)_{p-1} - \lim_{M\to\infty} \sum_{p=1}^{M} (1-\frac{\chi_p}{n})g(\varrho,\tau) \\
&= (D^{\eth}\psi)(\varrho,\tau) + R\psi(\varrho,\tau) + N\psi(\varrho,\tau) = g(\varrho,\tau) = 0
\end{aligned} \tag{4.4}$$

Finally, Eq. (4.4) proves that $\Theta(\varrho,\tau)$ satisfies the result of the original problem Eq. (3.1).

□

5. $q-$HASTM Solution of Fractional WBK Equation

The fractional Whitham-Broer-Kaup equations (1.2) with Caputo fractional derivative can be rewritten as

$$\begin{aligned} {}^{C}D_{\tau}^{\eth}\psi(\varrho,\tau)+\psi(\varrho,\tau)\,\tfrac{\partial\psi(\varrho,\tau)}{\partial\varrho}+\tfrac{\partial\nu(\varrho,\tau)}{\partial\varrho}+b\tfrac{\partial^2\psi(\varrho,\tau)}{\partial\varrho^2}=0,\\ {}^{C}D_{\tau}^{\eth}\nu(\varrho,\tau)+\nu(\varrho,\tau)\,\tfrac{\partial\psi(\varrho,\tau)}{\partial\varrho}+\psi(\varrho,\tau)\,\tfrac{\partial\nu(\varrho,\tau)}{\partial\varrho}+a\tfrac{\partial^3\psi(\varrho,\tau)}{\partial\varrho^3}-b\tfrac{\partial^2\nu(\varrho,\tau)}{\partial\varrho^2}=0, \end{aligned} \tag{5.1}$$

subject to initial conditions

$$\psi(\varrho,0)=f(\varrho),\qquad \nu(\varrho,0)=g(\varrho), \tag{5.2}$$

where $0<\eth\leq 1$ and ${}^{C}D_{\tau}{}^{\eth}$ present the Caputo fractional derivative of order $\eth$.
Taking the Shehu transform to equation (5.1) and on simplification, we get

$$\begin{aligned} &S[\psi(\varrho,\tau)]-\tfrac{\mu}{v}f(\varrho)+\left(\tfrac{\mu}{v}\right)^{\eth}\left\{\left[\psi(\varrho,\tau)\,\tfrac{\partial\psi(\varrho,\tau)}{\partial\varrho}+\tfrac{\partial\nu(\varrho,\tau)}{\partial\varrho}\right.\right.\\ &\qquad\left.\left.+\,b\tfrac{\partial^2\psi(\varrho,\tau)}{\partial\varrho^2}\right]\right\}=0,\\ &S[\nu(\varrho,\tau)]-\tfrac{\mu}{v}g(\varrho)+\left(\tfrac{\mu}{v}\right)^{\eth}\left\{\left[\nu(\varrho,\tau)\,\tfrac{\partial\psi(\varrho,\tau)}{\partial\varrho}+\psi(\varrho,\tau)\,\tfrac{\partial\nu(\varrho,\tau)}{\partial\varrho}\right.\right.\\ &\qquad\left.\left.+a\tfrac{\partial^3\psi(\varrho,\tau)}{\partial\varrho^3}-\,b\tfrac{\partial^2\nu(\varrho,\tau)}{\partial\varrho^2}\right]\right\}=0. \end{aligned} \tag{5.3}$$

Now, we define a non-linear operator as

$$\begin{aligned} &N^1[\Upsilon_1(\varrho,\tau;q),\Upsilon_2(\varrho,\tau;q)]=S[\Upsilon_1(\varrho,\tau;q)]-\tfrac{\mu}{v}f(\varrho)+\left(\tfrac{\mu}{v}\right)^{\eth}S[\Upsilon_1(\varrho,\tau;q)\\ &\qquad\times\tfrac{\partial\Upsilon_1(\varrho,\tau;q)}{\partial\varrho}+\tfrac{\partial\Upsilon_2(\varrho,\tau;q)}{\partial\varrho}+b\,\tfrac{\partial^2\Upsilon_1(\varrho,\tau;q)}{\partial\varrho^2}\Big],\\ &N^2[\Upsilon_1(\varrho,\tau;q),\Upsilon_2(\varrho,\tau;q)]=S[\Upsilon_2(\varrho,\tau;q)]-\tfrac{\mu}{v}g(\varrho)+\left(\tfrac{\mu}{v}\right)^{\eth}S[\Upsilon_2(\varrho,\tau;q)\\ &\qquad\times\tfrac{\partial\Upsilon_1(\varrho,\tau;q)}{\partial\varrho}+\Upsilon_1(\varrho,\tau;q)\,\tfrac{\partial\Upsilon_2(\varrho,\tau;q)}{\partial\varrho}+a\tfrac{\partial^3\Upsilon_1(\varrho,\tau;q)}{\partial\varrho^3}-b\,\tfrac{\partial^2\Upsilon_2(\varrho,\tau;q)}{\partial\varrho^2}\Big]. \end{aligned} \tag{5.4}$$

here $q\in\left[0,\frac{1}{n}\right]$ is an embedding parameter. Liao [25, 26] constructed zeroth-order deformation equation such as

$$\begin{aligned} (1-nq)\,S[\Upsilon_1(\varrho,\tau;q)-\psi(\varrho,0)]&=\hbar H(\varrho,\tau)\,N^1[\Upsilon_1(\varrho,\tau;q),\Upsilon_2(\varrho,\tau;q)],\\ (1-nq)\,S[\Upsilon_2(\varrho,\tau;q)-\nu(\varrho,0)]&=\hbar H(\varrho,\tau)\,N^2[\Upsilon_1(\varrho,\tau;q),\Upsilon_2(\varrho,\tau;q)]. \end{aligned} \tag{5.5}$$

here, S represent the Shehu transform, $\hbar$ is nonzero auxiliary parameter, $H(\varrho,\tau)\neq 0$ denoted an auxiliary function, $\psi(\varrho,0)$ and $\nu(\varrho,0)$ indicates initial guesses of $\psi(\varrho,\tau)$ and $\nu(\varrho,\tau)$, respectively. Let $q=0$ and $q=1$ in equation (5.5), we get

$$\begin{aligned} \Upsilon_1(\varrho,\tau;q)&=\psi_0(\varrho,\tau), & \Upsilon_1\left(\varrho,\tau;\tfrac{1}{n}\right)&=\psi(\varrho,\tau),\\ \Upsilon_2(\varrho,\tau;q)&=\nu_0(\varrho,\tau), & \Upsilon_2\left(\varrho,\tau;\tfrac{1}{n}\right)&=\nu(\varrho,\tau). \end{aligned} \tag{5.6}$$

Thus, if q increase from 0 to $\frac{1}{n}$, then $\Upsilon_1(\varrho,\tau;q)$ varies from initial guess $\psi_0(\varrho,\tau)$ to the solution $\psi(\varrho,\tau)$, and $\Upsilon_2(\varrho,\tau;q)$ varies from initial guess $\nu_0(\varrho,\tau)$ to the solution $\nu(\varrho,\tau)$, respectively. Upon expanding $\Upsilon_1(\varrho,\tau;q)$ and $\Upsilon_2(\varrho,\tau;q)$ according to Taylor's series near q, we have

$$\begin{aligned} \Upsilon_1(\varrho,\tau;q)&=\psi_0(\varrho,\tau)+\sum_{p=1}^{\infty}\psi_p(\varrho,\tau)\,q^p,\\ \Upsilon_2(\varrho,\tau;q)&=\nu_0(\varrho,\tau)+\sum_{p=1}^{\infty}\nu_p(\varrho,\tau)\,q^p, \end{aligned} \tag{5.7}$$

where

$$\begin{aligned} \psi_p(\varrho,\tau)&=\tfrac{1}{p!}\tfrac{\partial^p\Upsilon_1(\varrho,\tau;q)}{\partial q^p}\Big|_{q=0},\\ \nu_p(\varrho,\tau)&=\tfrac{1}{p!}\tfrac{\partial^p\Upsilon_2(\varrho,\tau;q)}{\partial q^p}\Big|_{q=0}. \end{aligned} \tag{5.8}$$

By proper choosing of $\psi_0(\varrho,\tau)$, $\nu_0(\varrho,\tau)$, $\hbar$, and $H(\varrho,\tau)$, the series in equation (5.7) converges at q = $\frac{1}{n}$, we will get

$$\begin{aligned}\psi(\varrho,\tau) &= \psi_0(\varrho,\tau) + \sum_{p=1}^{\infty} \psi_p(\varrho,\tau)\ \left(\tfrac{1}{n}\right)^p,\\ \nu(\varrho,\tau) &= \nu_0(\varrho,\tau) + \sum_{p=1}^{\infty} \nu_p(\varrho,\tau)\ \left(\tfrac{1}{n}\right)^p.\end{aligned} \tag{5.9}$$

We define the vectors $\overrightarrow{\psi_p}(\varrho,\tau)$, and $\overrightarrow{\nu_p}(\varrho,\tau)$ as

$$\begin{aligned}\overrightarrow{\psi_p}(\varrho,\tau) &= \{\psi_0(\varrho,\tau),\ \psi_1(\varrho,\tau),\ .....,\ \psi_p(\varrho,\tau)\},\\ \overrightarrow{\nu_p}(\varrho,\tau) &= \{\nu_0(\varrho,\tau),\ \nu_1(\varrho,\tau),\ .....,\ \nu_p(\varrho,\tau)\}.\end{aligned} \tag{5.10}$$

First, differentiating equation (5.5) p- times with respect to q, then evaluate at q = 0 and finally dividing by $\Gamma(p+1)$, we get

$$\begin{aligned}S[\psi_p(\varrho,\tau) - \chi_p\psi_{p-1}(\varrho,\tau)] &= \hbar H(\varrho,\tau)\, R_{1,p}\left[\overrightarrow{\psi}_{p-1}, \overrightarrow{\nu}_{p-1}\right],\\ S[\nu_p(\varrho,\tau) - \chi_p\nu_{p-1}(\varrho,\tau)] &= \hbar H(\varrho,\tau)\, R_{2,p}\left[\overrightarrow{\psi}_{p-1}, \overrightarrow{\nu}_{p-1}\right],\end{aligned} \tag{5.11}$$

where,

$$\begin{aligned}R_{1,p}\left[\overrightarrow{\psi}_{p-1}, \overrightarrow{\nu}_{p-1}\right] &= S[\psi_{p-1}(\varrho,\tau)] - \left(1-\tfrac{\chi_p}{n}\right)\tfrac{\mu}{v}[f(\varrho)]\\ &\quad +\left(\tfrac{\mu}{v}\right)^{\eth} S\left[\sum_{k=0}^{p-1}\psi_k\tfrac{\partial\psi_{p-1-k}}{\partial\varrho} + \tfrac{\partial\nu_{p-1}}{\partial\varrho} + b\tfrac{\partial^2\psi_{p-1}}{\partial\varrho^2}\right],\\ R_{2,p}\left[\overrightarrow{\psi}_{p-1}, \overrightarrow{\nu}_{p-1}\right] &= S[\nu_{p-1}(\varrho,\tau)] - \left(1-\tfrac{\chi_p}{n}\right)\tfrac{\mu}{v}[g(\varrho)]\\ &\quad +\left(\tfrac{\mu}{v}\right)^{\eth} S\left[\sum_{k=0}^{p-1}\psi_k\tfrac{\partial\nu_{p-1-k}}{\partial\varrho} + \sum_{k=0}^{p-1}\nu_k\tfrac{\partial\psi_{p-1-k}}{\partial\varrho} + a\tfrac{\partial^3\psi_{p-1}}{\partial\varrho^3} - b\tfrac{\partial^2\nu_{p-1}}{\partial\varrho^2}\right],\end{aligned} \tag{5.12}$$

and

$$\chi_p = \begin{cases} 0, & p \le 1\\ n, & otherwise\ . \end{cases} \tag{5.13}$$

Next, applying inverse ST to both sides of equation (5.11) and $H(\varrho,\tau) = 1$, we get

$$\begin{aligned}\psi_p(\varrho,\tau) &= \chi_p\psi_{p-1}(\varrho,\tau) + S^{-1}\left[\hbar R_{1,p}\left[\overrightarrow{\psi}_{p-1}, \overrightarrow{\nu}_{p-1}\right]\right],\\ \nu_p(\varrho,\tau) &= \chi_p\nu_{p-1}(\varrho,\tau) + S^{-1}\left[\hbar R_{2,p}\left[\overrightarrow{\psi}_{p-1}, \overrightarrow{\nu}_{p-1}\right]\right].\end{aligned} \tag{5.14}$$

Finally, we compute $\psi_p(\varrho,\tau)$ by using equation (5.14) for $p \ge 1$. Hence the M^{th} order approximate solution of equation (5.1) can be represented as

$$\begin{aligned}\psi(\varrho,\tau) &= \psi_0(\varrho,\tau) + \sum_{p=1}^{M} \psi_p(\varrho,\tau)\ \left(\tfrac{1}{n}\right)^p,\\ \nu(\varrho,\tau) &= \nu_0(\varrho,\tau) + \sum_{p=1}^{M} \nu_p(\varrho,\tau)\ \left(\tfrac{1}{n}\right)^p.\end{aligned} \tag{5.15}$$

Moreover, for $M \to \infty$, we get

$$\begin{aligned}\psi(\varrho,\tau) &= \psi_0(\varrho,\tau) + \sum_{p=1}^{\infty} \psi_p(\varrho,\tau)\ \left(\tfrac{1}{n}\right)^p,\\ \nu(\varrho,\tau) &= \nu_0(\varrho,\tau) + \sum_{p=1}^{\infty} \nu_p(\varrho,\tau)\ \left(\tfrac{1}{n}\right)^p.\end{aligned} \tag{5.16}$$

6. Applications of Fractional WBK equation

Example 1 If $a = 0$ and $b = \frac{1}{2}$, then the fractional WBK equation (1.2) reduces to the approximate long wave (ALW) equation [16, 41]

$$\begin{aligned} {}^{C}D_{\tau}^{\eth}\psi(\varrho,\tau) + \psi(\varrho,\tau)\,\tfrac{\partial\psi(\varrho,\tau)}{\partial\varrho} + \tfrac{\partial\nu(\varrho,\tau)}{\partial\varrho} + \tfrac{1}{2}\tfrac{\partial^2\psi(\varrho,\tau)}{\partial\varrho^2} = 0,\\ {}^{C}D_{\tau}^{\eth}\nu(\varrho,\tau) + \nu(\varrho,\tau)\,\tfrac{\partial\psi(\varrho,\tau)}{\partial\varrho} + \psi(\varrho,\tau)\,\tfrac{\partial\nu(\varrho,\tau)}{\partial\varrho} - \tfrac{1}{2}\tfrac{\partial^2\nu(\varrho,\tau)}{\partial\varrho^2} = 0, \end{aligned} \tag{6.1}$$

subject to initial conditions

$$\begin{aligned} \psi(\varrho,0) &= \theta - \kappa_1 \coth\left[\kappa_1(\varrho+\iota)\right],\\ \nu(\varrho,0) &= -{\kappa_1}^2 \mathrm{csch}^2\left[\kappa_1(\varrho+\iota)\right]. \end{aligned} \tag{6.2}$$

According to Eqs. (5.12)-(5.14), we get following results

$$\begin{aligned} \psi_0(\varrho,\tau) &= \theta - \kappa_1 \coth\left(\kappa_1(\varrho+\iota)\right),\\ \nu_0(\varrho,\tau) &= -{\kappa_1}^2 \mathrm{csch}^2\left(\kappa_1(\varrho+\iota)\right),\\ \psi_1(\varrho,\tau) &= \hbar\,\theta\,{\kappa_1}^2 \mathrm{csch}^2\left(\kappa_1(\varrho+\iota)\right)\tfrac{\tau^{\eth}}{\Gamma(\eth+1)},\\ \nu_1(\varrho,\tau) &= 2\,\hbar\,{\kappa_1}^3\,\theta \mathrm{csch}^2\left(\kappa_1(\varrho+\iota)\right)\coth\left(\kappa_1(\varrho+\iota)\right)\tfrac{\tau^{\eth}}{\Gamma(\eth+1)},\\ \psi_2(\varrho,\tau) &= \hbar(n+\hbar)\;\theta\,{\kappa_1}^2 \mathrm{csch}^2\left(\kappa_1(\varrho+\iota)\right)\tfrac{\tau^{\eth}}{\Gamma(\eth+1)}\\ &\quad - 2\,\hbar^2\,\theta^2\,{\kappa_1}^3 \mathrm{csch}^2\left(\kappa_1(\varrho+\iota)\right)\coth\left(\kappa_1(\varrho+\iota)\right)\tfrac{\tau^{2\eth}}{\Gamma(2\eth+1)},\\ \nu_2(\varrho,\tau) &= 2\,\hbar(n+\hbar)\;\theta\;{\kappa_1}^3 \mathrm{csch}^2\left(\kappa_1(\varrho+\iota)\right)\coth\left(\kappa_1(\varrho+\iota)\right)\tfrac{\tau^{\eth}}{\Gamma(\eth+1)}\\ &\quad - 2\,\hbar^2\,\theta^2\,{\kappa_1}^4 \mathrm{csch}^2\left(\kappa_1(\varrho+\iota)\right)\left(2+3\mathrm{csch}^2\left(\kappa_1(\varrho+\iota)\right)\right)\tfrac{\tau^{2\eth}}{\Gamma(2\eth+1)}, \end{aligned}$$

and so on.
If we set $n = 1$, $\eth = 1$ and $\hbar = -1$, then the solutions of (6.1) can be written as

$$\begin{aligned} \psi_{(M)}(\varrho,\tau) &= \sum_{p=0}^{M} \psi_p(\varrho,\tau)\,\left(\tfrac{1}{n}\right)^p,\\ \nu_{(M)}(\varrho,\tau) &= \sum_{p=0}^{M} \nu_p(\varrho,\tau)\,\left(\tfrac{1}{n}\right)^p, \end{aligned} \tag{6.3}$$

When $M \to \infty$, then solutions (6.3) converges to exact solution of (6.1)

$$\begin{aligned} \psi(\varrho,\tau) &= \theta - \kappa_1 \coth\left(\kappa_1(\eth - \theta\tau)\right),\\ \nu(\varrho,\tau) &= -{\kappa_1}^2 \operatorname{csc} h^2(\kappa_1(\eth - \theta\tau)). \end{aligned} \tag{6.4}$$

Example 2 If $a = 1$ and $b = 0$, then the fractional WBK equation (1.2) reduces to the modified Boussinesq equation [16, 41]

$$\begin{aligned} {}^{C}D_{\tau}^{\eth}\psi(\varrho,\tau) + \psi(\varrho,\tau)\,\tfrac{\partial\psi(\varrho,\tau)}{\partial\varrho} + \tfrac{\partial\nu(\varrho,\tau)}{\partial\varrho} = 0,\\ {}^{C}D_{\tau}^{\eth}\nu(\varrho,\tau) + \nu(\varrho,\tau)\,\tfrac{\partial\psi(\varrho,\tau)}{\partial\varrho} + \psi(\varrho,\tau)\,\tfrac{\partial\nu(\varrho,\tau)}{\partial\varrho} + \tfrac{\partial^3\nu(\varrho,\tau)}{\partial\varrho^3} = 0, \end{aligned} \tag{6.5}$$

subject to initial conditions

$$\begin{aligned} \psi(\varrho,0) &= \theta - 2\kappa_1 \coth\left[\kappa_1(\varrho+\iota)\right],\\ \nu(\varrho,0) &= -2{\kappa_1}^2 \mathrm{csch}^2\left[\kappa_1(\varrho+\iota)\right]. \end{aligned} \tag{6.6}$$

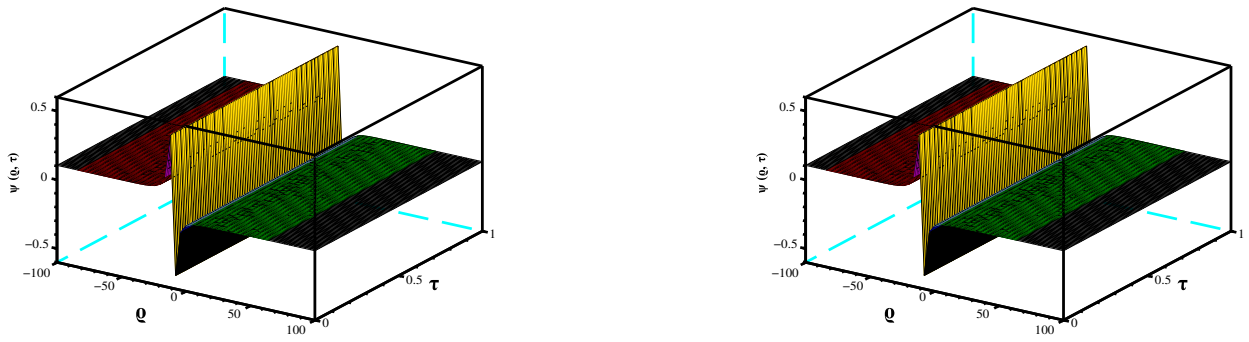

(a) Approximate solution of $\psi(\varrho, \tau)$ (b) Exact solution of $\psi(\varrho, \tau)$

Figure 1: $3-D$ plot of approximate Vs exact solutions of $\psi(\varrho, \tau)$ for **example 1** at $\eth = 1$, $\theta = 0.005$, $\kappa_1 = 0.10$, $\iota = 10$, $n = 1$ and $\hbar = -1$.

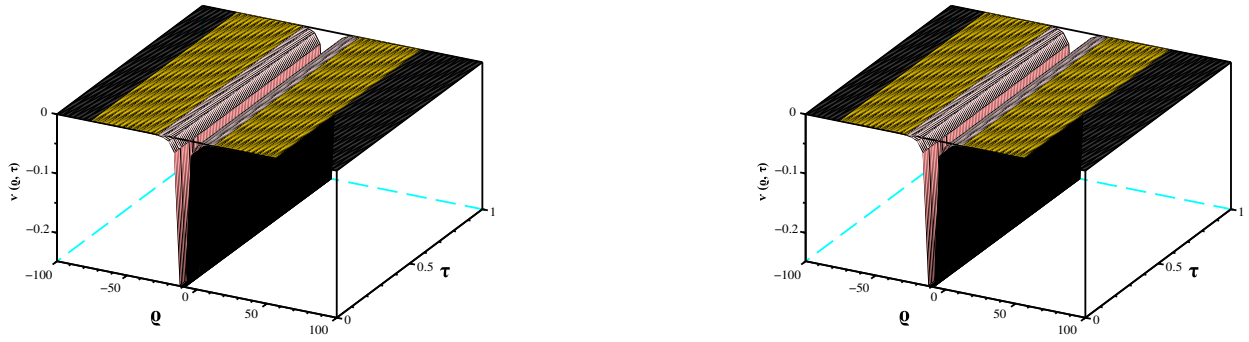

(a) Approximate solution of $\nu(\varrho, \tau)$ (b) Exact solution of $\nu(\varrho, \tau)$

Figure 2: $3-D$ plot of approximate Vs exact solutions of $\nu(\varrho, \tau)$ for **example 1** at $\eth = 1$, $\theta = 0.005$, $\kappa_1 = 0.10$, $\iota = 10$, $n = 1$ and $\hbar = -1$.

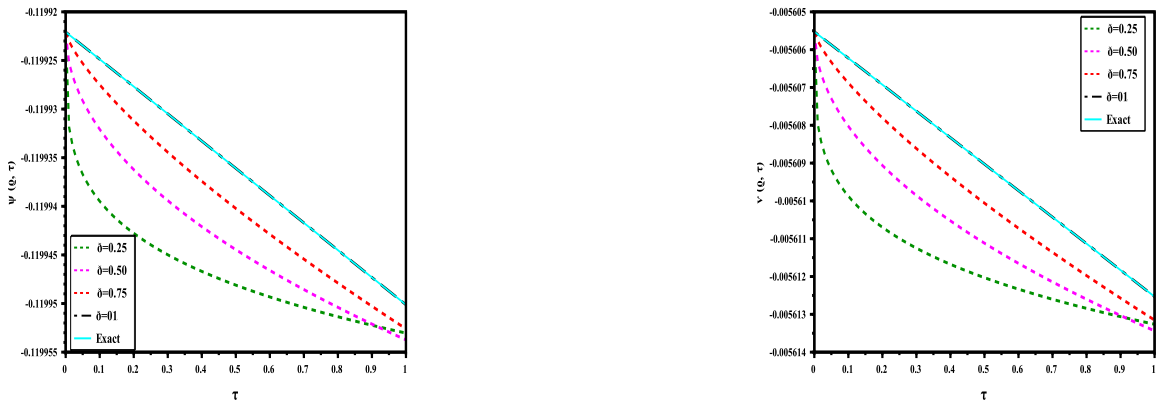

Figure 3: Impact of order $\eth$ on analytical and exact solution of **example 1** with $\theta = 0.005$, $\kappa_1 = 0.10$, $\iota = 10$, $n = 1$, $\varrho = 1$ and $\hbar = -1$.

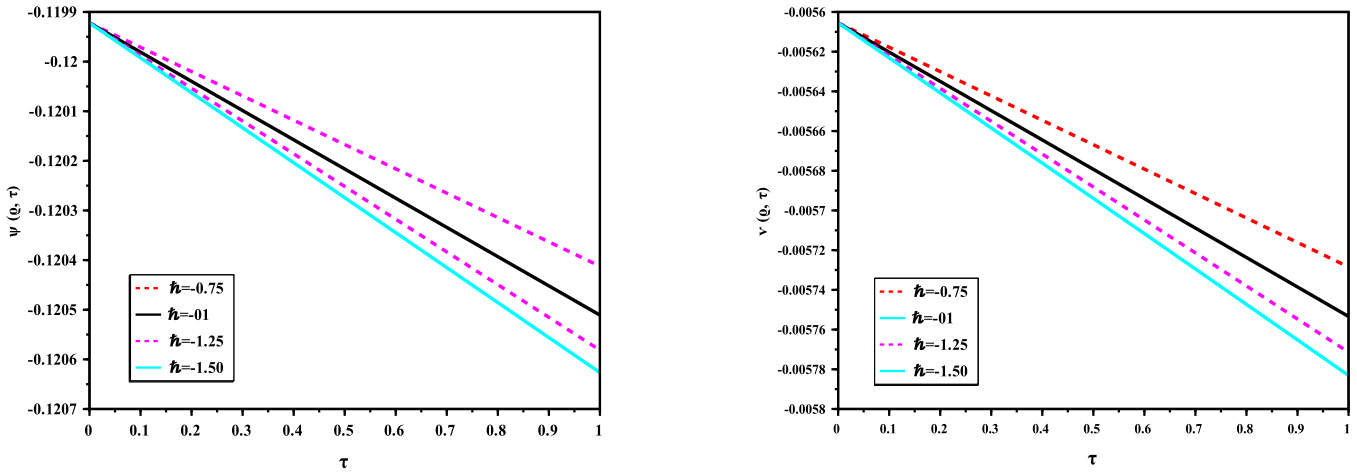

Figure 4: $2-D$ behaviour of (6.1) with distinct $\hbar$, when $\theta = 0.005$, $\kappa_1 = 0.10$, $\iota = 10$, $n = 5$ and $\varrho = 1$.

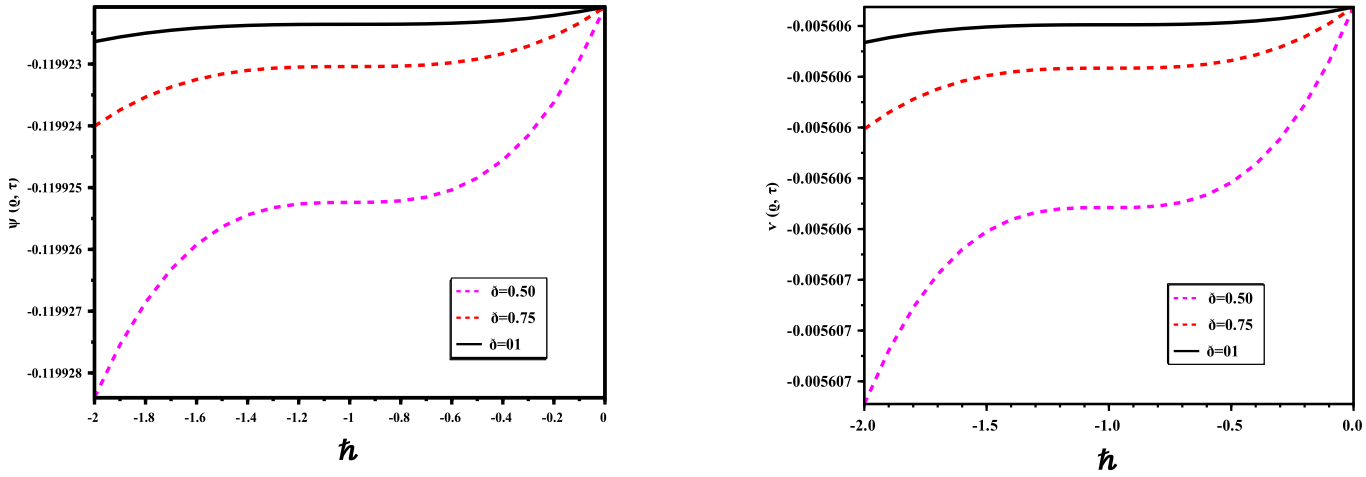

Figure 5: $\hbar$ curves of **example 1** with distinct $\eth$, when $\theta = 0.005$, $\kappa_1 = 0.10$, $\iota = 10$, $n = 1$, $\varrho = 1$ and $\tau = 0.01$.

Table I: Comparative analysis between OHAM, ADM, VIM, RPSM and q-HASTM for $\psi(\varrho,\tau)$ at $\hbar$ = - 1, $n=1$, $\iota=10$, $\theta=0.005$, $\kappa_1=0.10$ of example 1.

(ϱ,t)	$\lvert\psi_{Exa.}-\psi_{OHAM}\rvert$	$\lvert\psi_{Exa.}-\psi_{ADM}\rvert$	$\lvert\psi_{Exa.}-\psi_{VIM}\rvert$	$\lvert\psi_{Exa.}-\psi_{RPSM}\rvert$	$\lvert\psi_{Exa.}-\psi_{q-HASTM}\rvert$
$(0.1,0.1)$	3.17634×10^{-5}	8.02989×10^{-6}	3.17634×10^{-5}	6.73913×10^{-18}	6.73913×10^{-18}
$(0.1,0.3)$	9.54269×10^{-5}	7.38281×10^{-6}	9.54273×10^{-5}	1.08892×10^{-17}	1.08892×10^{-17}
$(0.1,0.5)$	1.59274×10^{-4}	6.79923×10^{-6}	1.59274×10^{-4}	1.12040×10^{-18}	1.12040×10^{-18}
$(0.2,0.1)$	3.09465×10^{-5}	3.23228×10^{-5}	3.09466×10^{-5}	4.72239×10^{-18}	4.72239×10^{-18}
$(0.2,0.3)$	9.29723×10^{-5}	2.97172×10^{-5}	$9,29725\times10^{-5}$	7.10655×10^{-18}	7.10655×10^{-18}
$(0.2,0.5)$	1.55176×10^{-4}	2.73673×10^{-5}	1.55176×10^{-4}	1.00389×10^{-17}	1.00389×10^{-17}
$(0.3,0.1)$	3.01549×10^{-5}	7.32051×10^{-5}	3.01549×10^{-5}	2.12448×10^{-17}	2.12448×10^{-17}
$(0.3,0.3)$	9.05932×10^{-5}	6.73006×10^{-5}	9.05935×10^{-5}	1.44235×10^{-17}	1.44235×10^{-17}
$(0.3,0.5)$	1.51204×10^{-4}	6.19760×10^{-5}	1.51204×10^{-4}	1.06299×10^{-17}	1.06299×10^{-17}
$(0.4,0.1)$	2.93874×10^{-5}	1.31032×10^{-4}	2.93874×10^{-5}	4.36379×10^{-17}	4.36379×10^{-17}
$(0.4,0.3)$	8.82870×10^{-5}	1.20455×10^{-4}	8.82871×10^{-5}	3.95777×10^{-17}	3.95777×10^{-17}
$(0.4,0.5)$	1.47354×10^{-4}	1.10919×10^{-4}	1.47354×10^{-4}	3.40839×10^{-17}	3.40839×10^{-17}
$(0.5,0.1)$	2.86432×10^{-5}	2.06186×10^{-4}	2.86433×10^{-5}	2.05053×10^{-18}	2.05053×10^{-18}
$(0.5,0.3)$	8.60506×10^{-5}	1.89528×10^{-4}	8.60509×10^{-5}	5.94932×10^{-17}	5.94932×10^{-17}
$(0.5,0.5)$	1.43620×10^{-4}	1.74510×10^{-4}	1.43620×10^{-4}	3.02966×10^{-17}	3.02966×10^{-17}

Table II: Comparative analysis between OHAM, ADM, VIM, RPSM and q-HASTM for $\nu(\varrho,\tau)$ at $\hbar$ = - 1, $n=1$, $\iota=10$, $\theta=0.005$, $\kappa_1=0.10$ of example 1.

(ϱ,t)	$\lvert\psi_{Exa.}-\psi_{OHAM}\rvert$	$\lvert\psi_{Exa.}-\psi_{ADM}\rvert$	$\lvert\psi_{Exa.}-\psi_{VIM}\rvert$	$\lvert\psi_{Exa.}-\psi_{RPSM}\rvert$	$\lvert\psi_{Exa.}-\psi_{q-HASTM}\rvert$
$(0.1,0.1)$	8.29711×10^{-6}	4.81902×10^{-4}	8.29711×10^{-6}	1.58608×10^{-18}	1.58608×10^{-18}
$(0.1,0.3)$	2.49346×10^{-5}	4.50818×10^{-4}	2.49346×10^{-5}	5.43944×10^{-19}	5.43944×10^{-19}
$(0.1,0.5)$	4.16299×10^{-5}	4.22221×10^{-4}	4.16299×10^{-5}	1.36881×10^{-18}	1.36881×10^{-18}
$(0.2,0.1)$	8.04063×10^{-6}	9.76644×10^{-4}	8.04063×10^{-6}	1.21449×10^{-18}	1.21449×10^{-18}
$(0.2,0.3)$	2.41634×10^{-5}	9.13502×10^{-4}	2.41634×10^{-5}	1.68513×10^{-19}	1.68513×10^{-19}
$(0.2,0.5)$	4.03419×10^{-5}	8.55426×10^{-4}	4.03419×10^{-5}	1.75768×10^{-18}	1.75768×10^{-18}
$(0.3,0.1)$	7.79401×10^{-6}	1.48482×10^{-3}	7.79401×10^{-6}	5.93717×10^{-19}	5.93717×10^{-19}
$(0.3,0.3)$	2.34220×10^{-5}	1.38858×10^{-3}	2.34220×10^{-5}	4.17842×10^{-19}	4.17842×10^{-19}
$(0.3,0.5)$	3.91034×10^{-5}	1.30009×10^{-3}	3.91034×10^{-5}	2.11323×10^{-18}	2.11323×10^{-18}
$(0.4,0.1)$	7.55675×10^{-6}	2.00705×10^{-3}	7.55675×10^{-6}	1.70872×10^{-18}	1.70872×10^{-18}
$(0.4,0.3)$	2.27087×10^{-5}	1.87661×10^{-3}	2.27087×10^{-5}	1.89994×10^{-18}	1.89994×10^{-18}
$(0.4,0.5)$	3.79121×10^{-5}	1.75670×10^{-3}	3.79121×10^{-5}	1.08612×10^{-18}	1.08612×10^{-18}
$(0.5,0.1)$	7.32847×10^{-6}	2.54396×10^{-3}	7.32847×10^{-6}	3.88866×10^{-18}	3.88866×10^{-18}
$(0.5,0.3)$	2.20224×10^{-5}	2.37815×10^{-3}	2.20224×10^{-5}	9.10368×10^{-18}	9.10368×10^{-18}
$(0.5,0.5)$	3.67658×10^{-5}	2.22578×10^{-3}	3.67658×10^{-5}	2.09445×10^{-18}	2.09445×10^{-18}

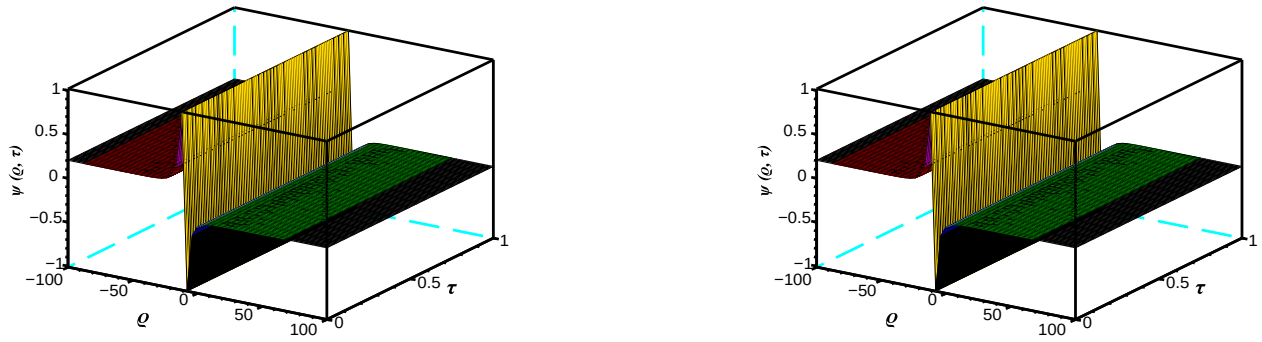

(a) Approximate solution of $\psi(\varrho,\tau)$ (b) Exact solution of $\psi(\varrho,\tau)$

Figure 6: $3-D$ plot of approximate Vs exact solutions of $\psi(\varrho,\tau)$ for **example 2** at $\eth = 1$, $\theta = 0.005$, $\kappa_1 = 0.10$, $\iota = 10$, $n = 1$ and $\hbar = -1$.

According to Eqs. (5.12)-(5.14), we get following results

$$\begin{aligned}
\psi_0(\varrho,\tau) &= \theta - 2\kappa_1 \coth(\kappa_1(\varrho+\iota)),\\
\nu_0(\varrho,\tau) &= -2\kappa_1{}^2 \operatorname{csch}^2(\kappa_1(\varrho+\iota)),\\
\psi_1(\varrho,\tau) &= 2\hbar\theta\kappa_1{}^2 \operatorname{csch}^2(\kappa_1(\varrho+\iota))\tfrac{\tau^{\eth}}{\Gamma(\eth+1)},\\
\nu_1(\varrho,\tau) &= 4\hbar\kappa_1{}^3\theta \operatorname{csch}^2(\kappa_1(\varrho+\iota))\coth(\kappa_1(\varrho+\iota))\tfrac{\tau^{\eth}}{\Gamma(\eth+1)},\\
\psi_2(\varrho,\tau) &= 2\hbar(n+\hbar)\ \theta\kappa_1{}^2 \operatorname{csch}^2(\kappa_1(\varrho+\iota))\ \tfrac{\tau^{\eth}}{\Gamma(\eth+1)}\\
&\quad - 4\hbar^2\theta^2\kappa_1{}^3 \operatorname{csch}^2(\kappa_1(\varrho+\iota))\coth(\kappa_1(\varrho+\iota))\tfrac{\tau^{2\eth}}{\Gamma(2\eth+1)},\\
\nu_2(\varrho,\tau) &= 4\hbar(n+\hbar)\ \theta\ \kappa_1{}^3 \operatorname{csch}^2(\kappa_1(\varrho+\iota))\coth(\kappa_1(\varrho+\iota))\tfrac{\tau^{\eth}}{\Gamma(\eth+1)}\\
&\quad - 4\hbar^2\theta^2\kappa_1{}^4 \operatorname{csch}^2(\kappa_1(\varrho+\iota))\left(2+3\operatorname{csch}^2(\kappa_1(\varrho+\iota))\right)\tfrac{\tau^{2\eth}}{\Gamma(2\eth+1)},
\end{aligned}$$

and so on.
If we set $n = 1$, $\eth = 1$ and $\hbar = -1$, then the solutions of (6.5) can be written as

$$\begin{aligned}
\psi_{(M)}(\varrho,\tau) &= \sum_{p=0}^{M} \psi_p(\varrho,\tau)\ \left(\tfrac{1}{n}\right)^p,\\
\nu_{(M)}(\varrho,\tau) &= \sum_{p=0}^{M} \nu_p(\varrho,\tau)\ \left(\tfrac{1}{n}\right)^p,
\end{aligned} \tag{6.7}$$

When $M \to \infty$, then solutions (6.7) converges to exact solution of (6.5)

$$\begin{aligned}
\psi(\varrho,\tau) &= \theta - 2\kappa_1 \coth(\kappa_1(\eth-\theta\tau)),\\
\nu(\varrho,\tau) &= -2\kappa_1{}^2 \operatorname{csc} h^2(\kappa_1(\eth-\theta\tau)).
\end{aligned} \tag{6.8}$$

7. Results and Discussions

The numerical results reported in Tables 1–4 display the absolute errors corresponding to the values $\eth = 1$, $\hbar = -1$, $n = 1$, $\iota = 10$, $\theta = 0.005$, $\kappa_1 = 0.10$. The obtained results confirm that the proposed method (q-HASTM) exhibits superior accuracy when compared to several established techniques available in the literature: [13, 16, 34, 41]. Figures 1-2 illustrates the comparative behavior between the analytical and exact solutions of equation (6.1), while figure 3 shows the 2-D nature of the approximate and

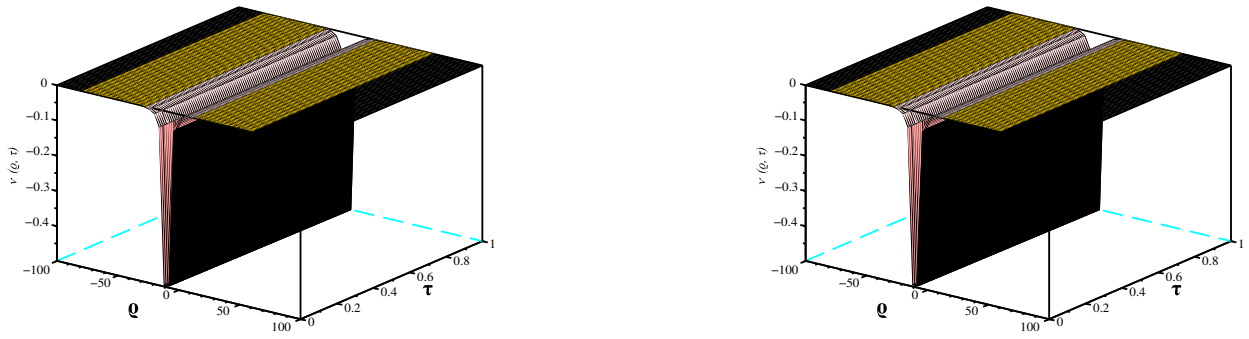

(a) Approximate solution of $\nu(\varrho, \tau)$ (b) Exact solution of $\nu(\varrho, \tau)$

Figure 7: $3-D$ plot of approximate Vs exact solutions of $\nu(\varrho, \tau)$ for **example 2** at $\eth = 1$, $\theta = 0.005$, $\kappa_1 = 0.10$, $\iota = 10$, $n = 1$ and $\hbar = -1$.

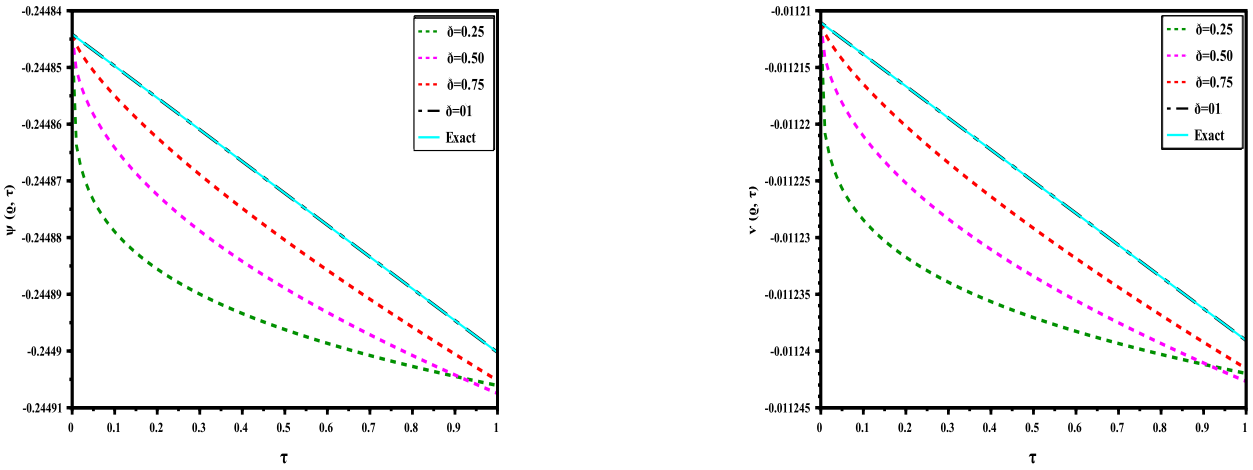

Figure 8: Impact of order $\eth$ on analytical and exact solution of **example 2** with $\theta = 0.005$, $\kappa_1 = 0.10$, $\iota = 10$, $n = 1$, $\varrho = 1$ and $\hbar = -1$.

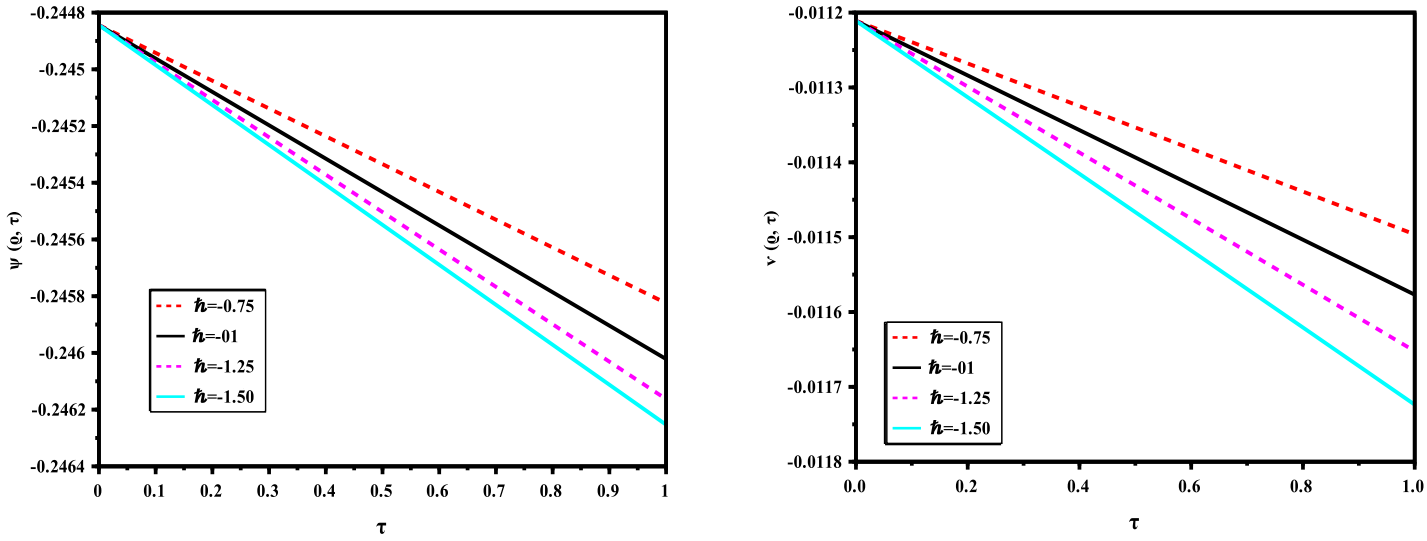

Figure 9: $2-D$ behaviour of (6.5) with distinct $\hbar$, when $\theta = 0.005$, $\kappa_1 = 0.10$, $\iota = 10$, $n = 5$ and $\varrho = 1$.

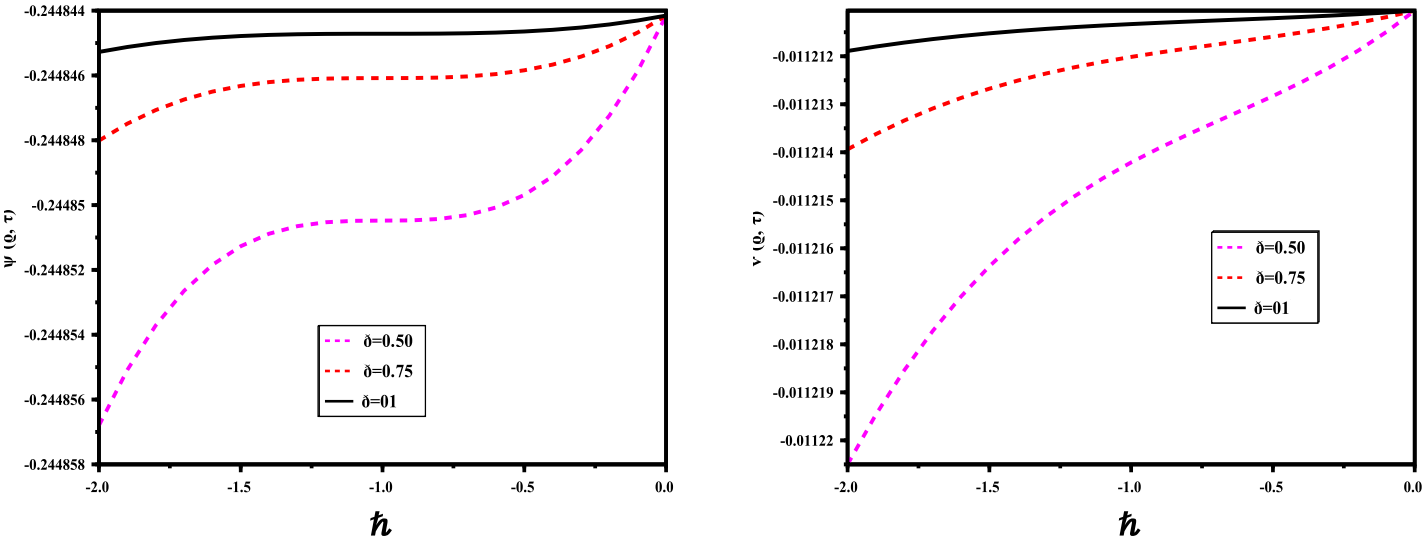

Figure 10: $\hbar$ curves of **example 2** with distinct $\eth$, when $\theta = 0.005$, $\kappa_1 = 0.10$, $\iota = 10$, $n = 1$, $\varrho = 1$ and $\tau = 0.01$.

Table III: Comparative analysis between OHAM, ADM, VIM, RPSM and q-HASTM for $\psi(\varrho,\tau)$ at $\hbar$ = -1, $n=1$, $\iota=10$, $\theta=0.005$, $\kappa_1=0.10$ of example 2.

(ϱ,t)	$\lvert\psi_{Exa.}-\psi_{OHAM}\rvert$	$\lvert\psi_{Exa.}-\psi_{ADM}\rvert$	$\lvert\psi_{Exa.}-\psi_{VIM}\rvert$	$\lvert\psi_{Exa.}-\psi_{RPSM}\rvert$	$\lvert\psi_{Exa.}-\psi_{q-HASTM}\rvert$
$(0.1,0.1)$	6.35267×10^{-5}	8.16297×10^{-7}	6.35267×10^{-5}	1.34780×10^{-17}	1.34780×10^{-17}
$(0.1,0.3)$	1.90854×10^{-4}	7.64245×10^{-7}	1.90854×10^{-4}	2.17823×10^{-17}	2.17823×10^{-17}
$(0.1,0.5)$	3.18548×10^{-4}	7.16083×10^{-7}	3.18548×10^{-4}	2.24972×10^{-18}	2.24972×10^{-18}
$(0.2,0.1)$	6.18930×10^{-5}	3.26243×10^{-6}	6.18930×10^{-5}	9.38089×10^{-18}	9.38089×10^{-18}
$(0.2,0.3)$	1.85945×10^{-4}	3.05458×10^{-6}	1.85945×10^{-4}	1.43996×10^{-17}	1.43996×10^{-17}
$(0.2,0.5)$	3.10352×10^{-4}	2.86226×10^{-6}	3.10352×10^{-4}	1.97731×10^{-17}	1.97731×10^{-17}
$(0.3,0.1)$	6.03095×10^{-5}	7.33445×10^{-6}	6.03095×10^{-5}	4.24677×10^{-17}	4.24677×10^{-17}
$(0.3,0.3)$	1.81187×10^{-4}	6.86758×10^{-6}	1.81187×10^{-4}	2.87822×10^{-17}	2.87822×10^{-17}
$(0.3,0.5)$	3.02408×10^{-4}	6.43557×10^{-6}	3.02408×10^{-4}	2.11487×10^{-17}	2.11487×10^{-17}
$(0.4,0.1)$	5.87746×10^{-5}	1.30286×10^{-5}	5.87746×10^{-5}	8.72342×10^{-17}	8.72342×10^{-17}
$(0.4,0.3)$	$1,76574\times10^{-4}$	1.22000×10^{-5}	$1,76574\times10^{-4}$	7.90451×10^{-17}	7.90451×10^{-17}
$(0.4,0.5)$	2.94707×10^{-4}	1.14333×10^{-5}	2.94707×10^{-4}	6.79998×10^{-17}	6.79998×10^{-17}
$(0.5,0.1)$	5.72867×10^{-4}	2.03415×10^{-5}	5.72867×10^{-4}	4.07931×10^{-18}	4.07931×10^{-18}
$(0.5,0.3)$	1.72102×10^{-4}	1.90489×10^{-5}	1.72102×10^{-4}	1.19703×10^{-17}	1.19703×10^{-17}
$(0.5,0.5)$	2.87241×10^{-4}	1.78528×10^{-5}	2.87241×10^{-4}	6.07085×10^{-17}	6.07085×10^{-17}

Table IV: Comparative analysis between OHAM, ADM, VIM, RPSM and q-HASTM for $\psi(\varrho,\tau)$ at $\hbar$ = -1, $n=1$, $\iota=10$, $\theta=0.005$, $\kappa_1=0.10$ of example 2.

(ϱ,t)	$\lvert\psi_{Exa.}-\psi_{OHAM}\rvert$	$\lvert\psi_{Exa.}-\psi_{ADM}\rvert$	$\lvert\psi_{Exa.}-\psi_{VIM}\rvert$	$\lvert\psi_{Exa.}-\psi_{RPSM}\rvert$	$\lvert\psi_{Exa.}-\psi_{q-HASTM}\rvert$
$(0.1,0.1)$	1.65942×10^{-5}	5.88676×10^{-5}	1.65942×10^{-5}	3.17215×10^{-18}	3.17215×10^{-18}
$(0.1,0.3)$	4.98691×10^{-5}	5.56914×10^{-5}	4.98691×10^{-5}	1.08813×10^{-18}	1.08813×10^{-18}
$(0.1,0.5)$	8.32598×10^{-5}	5.27169×10^{-5}	8.32598×10^{-5}	2.73648×10^{-18}	2.73648×10^{-18}
$(0.2,0.1)$	1.60813×10^{-5}	1.18213×10^{-4}	1.60813×10^{-5}	2.42893×10^{-18}	2.42893×10^{-18}
$(0.2,0.3)$	4.83269×10^{-5}	1.11833×10^{-4}	4.83269×10^{-5}	1.39638×10^{-18}	1.39638×10^{-18}
$(0.2,0.5)$	8.06837×10^{-5}	1.05858×10^{-4}	8.06837×10^{-5}	3.50926×10^{-18}	3.50926×10^{-18}
$(0.3,0.1)$	1.55880×10^{-5}	1.78041×10^{-4}	1.55880×10^{-5}	1.18742×10^{-18}	1.18742×10^{-18}
$(0.3,0.3)$	4.68440×10^{-5}	1.68429×10^{-4}	4.68440×10^{-5}	8.35230×10^{-19}	8.35230×10^{-19}
$(0.3,0.5)$	7.82068×10^{-5}	1.59428×10^{-4}	7.82068×10^{-5}	4.22825×10^{-18}	4.22825×10^{-18}
$(0.4,0.1)$	1.51135×10^{-5}	2.38356×10^{-4}	1.51135×10^{-5}	3.41750×10^{-18}	3.41750×10^{-18}
$(0.4,0.3)$	4.54174×10^{-5}	2.25483×10^{-4}	4.54174×10^{-5}	3.80156×10^{-18}	3.80156×10^{-18}
$(0.4,0.5)$	7.58243×10^{-5}	2.13430×10^{-4}	7.58243×10^{-5}	2.18005×10^{-18}	2.18005×10^{-18}
$(0.5,0.1)$	1.46569×10^{-5}	2.99162×10^{-4}	1.46569×10^{-5}	7.77731×10^{-18}	7.77731×10^{-18}
$(0.5,0.3)$	4.40448×10^{-5}	2.83001×10^{-4}	4.40448×10^{-5}	1.82067×10^{-18}	1.82067×10^{-18}
$(0.5,0.5)$	7.35317×10^{-5}	2.67868×10^{-4}	7.35317×10^{-5}	4.18858×10^{-18}	4.18858×10^{-18}

exact solutions of equation (6.1) for different values of $\eth$. Figure 4 presents the variation of the approximate solution with respect to different values of $\hbar$. Figure 5 demonstrates the $\hbar$-curves for (6.1) at $n = 1$, which help to control the convergence rate of the proposed method.
Additionally, figures 6-7 compares the approximate and exact solutions of equation (6.5) with $\eth = 1, \quad \hbar = -1, \quad n = 1, \quad \iota = 10, \quad \theta = 0.005, \quad \kappa_1 = 0.10$. Figures 8 examine the variation in approximate solution Vs exact solution for distinct values of $\eth$, while figure 9 present the impact of $\hbar$. Finally, Figure 10 depicts the behavior of the $\hbar$-curves associated with equation (6.5), offering further validation of the method's robustness across different parametric conditions.

8. Conclusions

In this study, the q-Homotopy Analysis Shehu Transform Method (q-HASTM) is employed to investigate the time-fractional coupled WBK equations. Analytical and numerical solutions are obtained for two specific cases: the fractional Approximate Long Wave (ALW) and Modified Boussinesq (MB) equations. The results highlight the efficiency and accuracy of the proposed approach. Notably, the method yields a convergent series solution with components that are straightforward to compute, without requiring perturbation techniques, linearization, or restrictive assumptions. Additionally, the influence of varying fractional-order values on the approximate solutions is examined, revealing that the method produces more precise and efficient results as the order approaches unity ($\eth \to 1$). The numerical and graphical findings affirm the computational reliability of q-HASTM, establishing it as an effective alternative for solving time-fractional linear and nonlinear differential equations. In the future, we intend solve some new fractional models, such as in [31, 9] and make comparisons with other numerical methods [31, 4, 9].

References

[1] P. Agarwal and A.A. El-sayed, *Non-standard finite difference and Chebyshev collocation methods for solving fractional diffusion equation*, Physica A **500** (2018), 40–49. 1

[2] A. Ali, K. Shah and R.A. Khan, *Numerical treatment for solving wave solution of fractional Whitham-Broer-Kaup equations*, Alex. Eng. J. **57**(3) (2018), 1991–2008. 1

[3] M. Amkadni, A. Azzouzi, and Z. Hammouch, *On the exact solutions of laminar MHD flow over a stretching flat plate*, Commun. Nonlinear Sci. Numer. Simul. **13**(2) (2008), 359–368. 1

[4] E. Ata and İ. Kıymaz, *Special functions with general kernel: Properties and applications to fractional partial differential equations*, Int. J. Math. Comput. Eng. **3**(2) (2024), 153–166. 1, 8

[5] D. Baleanu, Z.B. Guvenc and J.A.T. Machado, *New trends in nanotechnology and fractional calculus applications*, Springer **10** (2010), 978–990. 1

[6] D. Baleanu, G.C. Wu and S.D. Zeng, *Chaos analysis and asymptotic stability of generalized Caputo fractional differential equations*, Chaos Solitons Fractals **102** (2017), 99–105. 1

[7] H.M. Baskonus, Z. Hammouch, T. Mekkaoui, and H. Bulut, *Chaos in the fractional order logistic delay system: circuit realization and synchronization*, AIP Conf. Proc. **1738**(1) (2016), 290005. 1

[8] L.J. Broer, *Approximate equations for long water waves*, Appl. Sci. Res. **31** (1975), 377–395. 1

[9] M. Didgar, A. Vahidi and J. Biazar, *An Approximate Approach for Systems of Fractional Integro-Differential Equations Based on Taylor Expansion*, Kragujevac J. Math. **44**(3) (2020), 379–392. 1, 8

[10] C.S. Drapaca and S. Sivaloganathan, *A fractional model of continuum mechanics*, J. Elasticity **107** (2012), 105–123. 1

[11] R.S. Dubey, F.B.M. Belgacem and P. Goswami, *Homotopy perturbation approximate solutions for Bergman's minimal blood glucose-insulin model*, Fract. Geom. Nonlinear Anal. Med. Biol. **2**(3) (2016), 1–6. 1

[12] S.O. Edeki, O.P. Ogundile, B. Osoba, G.A. Adeyemi, F.O. Egara and A.S. Ejoh, *Coupled FCT-HP for analytical solutions of the generalized time-fractional Newell-Whitehead-Segel equation*, WSEAS Trans. Syst. Control **13** (2018), 266–274. 1

[13] M. El-Sayed and D. Kaya, *Exact and numerical travelling wave solutions of Whitham-Broer-Kaup equations*, Appl. Math. Comput. **167**(2) (2005), 1339–1349. 1, 7

[14] R. Faiz, W. Jamshed, S.S.U. Devi, M. Prakash, N.A.A.M. Nasir, Z. Hammouch, M.R. Eid, K.S. Nisar, A.B. Mahammed, A.H. Abdel-Aty, I.S. Yahia, and E.M. Eed, *Heat flow saturate of Ag/MgO-water hybrid nanofluid in heated trigonal enclosure with rotate cylindrical cavity by using Galerkin finite element*, Sci. Rep. **12**(1) (2022), 2302. 1

[15] S.M. Guo, L.Q. Mei, Y. Li and Y.F. Sun, *The improved fractional sub-equation method and its applications to the space-time fractional differential equations in fluid mechanics*, Phys. Lett. A **376**(4) (2012), 407–411. 1

[16] S. Haq and M. Ishaq, *Solution of coupled Whitham–Broer–Kaup equations using optimal homotopy asymptotic method*, Ocean Eng. **84** (2014), 81–88. 6, 6, 7
[17] H. Jafari, *A new general integral transform for solving integral equations*, J. Adv. Res. **32** (2021), 133–138. 1
[18] H. Jafari and S. Aggarwal, *Upadhyaya integral transform: A tool for solving non-linear Volterra integral equations*, Math. Comput. Sci. **5**(2) (2024), 63–71. 1
[19] H. Jafari, H. Tajadodi and Y. S. Gasimov, *Modern Computational Methods for Fractional Differential Equations*, Chapman and Hall/CRC (2025). 1
[20] D.J. Kaup, *A higher-order water-wave equation and the method for solving it*, Prog. Theor. Phys. **54** (1975), 396–408. 1
[21] Z.H. Khan and W.A. Khan, *N-transform-properties and applications*, NUST J. Eng. Sci. **1**(1) (2008), 127–133. 1
[22] S. Kumar, A. Kumar, S. Momani, M. Aldhaifallah and K.S. Nisar, *Numerical solutions of nonlinear fractional model arising in the appearance of the strip patterns in two dimensional systems*, Adv. Differ. Equ. **413** (2019), 1–19. 1
[23] D. Kumar and R. Prakash, *Numerical approximation of Newell-Whitehead-Segel equation of fractional order*, Nonlinear Eng. **5**(2) (2016), 81–86. 1
[24] D. Kumar, A.R. Seadwy and A.K. Joarder, *Modified Kudryashov method via new exact solutions for some conformable fractional differential equations arising in mathematical biology*, Chin. J. Phys. **56**(1) (2018), 75–85. 1
[25] S.J. Liao, *The proposed homotopy analysis technique for the solution of nonlinear problems*, PhD thesis, Shanghai Jiao Tong University, Shanghai, (1992). 5
[26] S.J. Liao, *An approximate solution technique not depending on small parameters: A special example*, Int. J. Non-Linear Mech. **30**(3) (1995), 371–380. 5
[27] S. Maitama and W. Zhao, New integral transform: Shehu transform a generalization of Sumudu and Laplace transform for solving differential equations, *arXiv* (2019) 11370. 2.3, 2.5
[28] S. Manjarekar and H. Jafari, *A modification on the new general integral transform*, Adv. Math. Models Appl. **7**(3) (2022), 253–263. 1, 2.2
[29] T. Mekkaoui and Z. Hammouch, *Approximate analytical solutions to the Bagley–Torvik equation by the Fractional Iteration Method*, Ann. Univ. Craiova Math. Comput. Sci. Ser. **39** (2012). 1
[30] H. Nasrolahpour, *A note on fractional electrodynamics*, Commun. Nonlinear Sci. Numer. Simul. **18**(9) (2013), 2589–2593. 1
[31] Z. Öztürk, H. Bilgil and S. Sorgun, *Fractional SAQ alcohol model: stability analysis and Türkiye application*, Int. J. Math. Comput. Eng. **3**(2) (2024), 125–136. 1, 8
[32] D.G. Prakasha, P. Veeresha and M.S. Rawashdeh, *Numerical solution for (2+1) dimensional time-fractional coupled Burger equation using fractional natural decomposition method*, Math. Methods Appl. Sci. **42**(10) (2019), 3409–3427. 1
[33] A. Prakash and V. Verma, *Numerical method for fractional model of Newell-Whitehead-Segel equation*, Front. Phys. **7**(15) (2019). 1
[34] M. Rafel and H. Daniali, *Application of the variational iteration method to the Whitham-Broer-Kaup equations*, Comput. Math. Appl. **54** (2007), 1079–1085. 1, 7
[35] R. Saadeh, M. Alaroud, M. Al-Smadi, R.R. Ahmad and U. Khair, *Application of fractional residual power series algorithm to solve Newell-Whitehead-Segel equation of fractional order*, Symmetry **11**(12) (2019), 1–13. 1
[36] M. Shrahili, R.S. Dubey and A. Shafay, *Inclusion of fading memory to Banister model of changes in physical condition*, Discrete Contin. Dyn. Syst. Ser. S **13**(3) (2020), 881–888. 1
[37] M. Sirajul and M. Ishaq, *Solution of coupled Whitham-Broer-Kaup equations using optimal homotopy asymptotic method*, Ocean Eng. **84** (2014), 81–108. 1
[38] M.F. Uddin, M.G. Hafez, Z. Hammouch, H. Rezazadeh, and D. Baleanu, *Traveling wave with beta derivative spatial-temporal evolution for describing the nonlinear directional couplers with metamaterials via two distinct methods*, Alex. Eng. J. **60**(1) (2021), 1055–1065. 1
[39] P. Veeresha and D.G. Prakasha, *An efficient technique for two-dimensional fractional order biological population model*, Int. J. Model. Simul. Sci. Comput. **11**(1) (2020). 1
[40] D. Vieru, C. Fetecau, N.A. Shah and S.J. Yook, *Unsteady natural convection flow due to fractional thermal transport and symmetric heat source/sink*, Alex. Eng. J. **64** (2023), 761–770. 1
[41] Y. Wang, Y.F. Zhang, Z. Jiang and M. Iqbal, *A fractional Whitham-Broer-Kaup equation and its possible application to tsunami prevention*, Therm. Sci. **21**(4) (2017), 1847-1855. 1, 6, 6, 7
[42] G.B. Whitham, *Variational methods and applications to water waves*, Proc. R. Soc. A **299** (1967), 6–25. 1
[43] L.K. Yadav, G. Agarwal, M.M. Gour and M. Kumari, *Analytical approach to study weakly nonlocal fractional Schrödinger equation via novel transform*, Int. J. Dyn. Control (2023). 1
[44] M. Zamir, F. Nadeem, T. Abdeljawad, and Z. Hammouch, *Threshold condition and non-pharmaceutical interventions' control strategies for elimination of COVID-19*, Results Phys. **20** (2021), 103698. 1